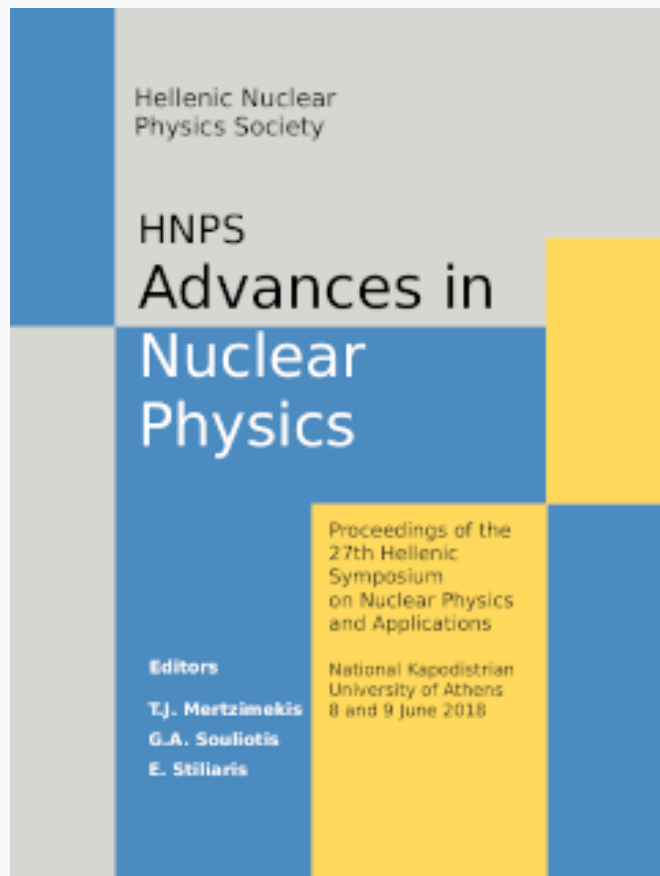


## HNPS Advances in Nuclear Physics

Vol 26 (2018)

HNPS2018



### Spallation of 56Fe by 1.0 GeV Protons

*N. G. Nicolis, G. S. Soulardis, A. Asimakopoulou*

doi: [10.12681/hnps.1791](https://doi.org/10.12681/hnps.1791)

### To cite this article:

Nicolis, N. G., Soulardis, G. S., & Asimakopoulou, A. (2019). Spallation of 56Fe by 1.0 GeV Protons. *HNPS Advances in Nuclear Physics*, 26, 25–30. <https://doi.org/10.12681/hnps.1791>

# Spallation of $^{56}\text{Fe}$ by 1.0 GeV Protons

N.G. Nicolis <sup>1,\*</sup>, G.A. Souliotis<sup>2</sup> and A. Asimakopoulou<sup>2</sup>

<sup>1</sup> Department of Physics, The University of Ioannina, Ioannina 45110, Greece

<sup>2</sup> Laboratory of Physical Chemistry, Department of Chemistry, University of Athens, Athens, Greece

---

**Abstract** Mass, charge and isotopic distributions observed in spallation reactions of  $^{56}\text{Fe}$  with 1 GeV protons are analysed in the framework of the intranuclear cascade code ISABEL coupled with the sequential binary decay code MECO. The code MECO provides a description of the equilibrated nuclear decay by the emission of gamma-rays, light-mass particles and clusters as well as intermediate mass fragments emitted in their ground, excited bound and excited unbound states (continuum) according to a generalized Weisskopf formalism. A good overall description of the experimental data is obtained with a global Fermi gas level density parameter and inverse cross sections based on the Christensen and Winther nuclear potential. Multifragmentation decay events are simulated with the code SMM and their influence on the above observables is discussed.

**Keywords** Nuclear reactions, Spallation, Intranuclear cascade model, Statistical model.

---

## INTRODUCTION

The study of nucleon-induced spallation reactions is a subject of extensive experimental and theoretical studies due to their importance in basic and applied Nuclear Science. Spallation reactions have numerous applications in accelerator-driven systems (ADS), transmutation of nuclear waste, spallation neutron sources and the production of rare isotopes [1]. Implications in astrophysics and space research are also important due to the interaction of cosmic rays with interstellar bodies and radiation damage of electronic devices in space [2]. Last but not least, this type of reactions provides a framework for testing high-energy nuclear reaction models in the bombarding energy range above 150-200 MeV [3].

A proton-induced spallation reaction (SR) proceeds in two stages. In the first stage, the incident particle interacts with the nucleons of the target in a sequence of collisions. As a result, we have the formation of an intranuclear cascade (INC) of high-energy (greater than 20 MeV) protons, neutrons and pions within the nucleus. This is a fast process lasting approximately  $10^{-22}\text{s}$ . During the intranuclear cascade, some of these energetic hadrons escape from the target. Others deposit their kinetic energy in the nucleus leaving it in an excited state. In the second stage, the produced excited nuclear species deexcite. Sequential evaporation is assumed to be the dominant process with a typical time scale of  $10^{-8}\text{s} - 10^{-6}\text{s}$ . Emission of nucleons, protons, alpha-particles and gamma-rays is dominant. Emission of heavier nucleon clusters in their ground or excited states is also possible. If the target is heavy enough, high-energy fission may compete with sequential evaporation. The deexcitation products of target-like and/or fission fragments may be radioactive. In the case of thick target experiments, the secondary high-energy particles produced in the INC phase move roughly in

---

\* Corresponding author, email: nnicolis@cc.uoi.gr

the same direction as the incident proton and induce secondary spallation reactions. In such a case, a hadronic cascade is observed as a result of an accumulation of all reactions initiated by the primary and secondary particles. In many applications it is desirable to have a reliable model description of the number of neutrons emitted in a spallation reaction, as well as associated observables like fission cross sections, mass and isotopic distributions of the reaction products.

The present work, concerns the description of a thin target experiment. We have initiated an extensive study of spallation reactions involving light and heavy targets. In the following, we report on the description of proton-induced spallation reactions on  $^{56}\text{Fe}$  at 1.0 GeV. We employ a phenomenological two-step approach in which we couple the results of an INC code evaporation codes incorporating the sequential binary decay with heavy fragments as well as a multifragmentation mechanism. The employed nuclear reaction codes are briefly discussed in Section II. In Section III, results of preliminary calculations are compared with experimental data consisting of mass, charge and isotopic distributions. Our results are summarized in the last Section.

## DESCRIPTION OF THE NUCLEAR REACTION CODES

For the description of the INC phase, we use the code ISABELE [4,5]. It is a well tested Monte-Carlo code with a long history of improvements. The target nucleus is simulated by a continuous medium bounded by a diffuse surface. Collisions between the incident nucleon and the nucleons of the target occur with a criterion based on the mean free path. Between successive collisions, linear trajectories are assumed. Free nucleon-nucleon cross sections are used. The code allows for elastic and inelastic N-N collisions. Furthermore, it takes full account of Pauli blocking i.e. interactions resulting in nucleon falling below the Fermi sea are forbidden. From a typical run we obtain the mass number (A), atomic number (Z) and excitation energy ( $E^*$ ) of the various nuclear species produced in the INC phase. The deexcitation stage is described with the codes SMM and MECO.

The SMM code [6-9] combines a description of sequential compound nucleus decay with a multifragmentation model. Equilibrium compound nucleus decay dominates at excitation energies  $E^* < 2-3$  MeV/A. At higher energies, the importance of these processes diminishes and multifragment decay takes over. The fission decay channel is taken into account empirically, by producing fission fragment mass distributions with parameters adjusted to fit experimental data [8]. At  $E^* > 4$  MeV/A, multifragmentation is expected to dominate. Thus, all possible decay processes occurring in the wide excitation energy range realized in a spallation reaction should be adequately taken into account.

The code MECO [10] is a multisequential binary decay code. It describes the equilibrium decay of excited nuclei as a sequence of binary division processes involving the emission of light particles, gamma rays and nucleon clusters in their ground, excited bound and unbound states. Emission of nucleons and progressively heavier clusters leading to symmetric mass divisions are calculated in a generalized Weisskopf evaporation formalism. The computational method is Monte-Carlo, thus allowing the simulation of experimental conditions. Also, it may accommodate any number of user-defined channels. MECO provides a complete description of compound nucleus decay of medium to low mass ( $A < 100$ ) systems and excitation energies  $E^* < 2-3$  MeV/A.

## COMPARISONS WITH EXPERIMENTAL DATA

In the following calculations with MECO, we use level densities described with the composite level density formula of Gilbert and Cameron. In the Fermi gas excitation energy region, we use an energy-independent level density constant  $a=A/8.0$  for all nuclei involved. Transmission coefficients for the emission of neutrons, protons and IMF's with a  $Z$  less than 5 were calculated with the optical model, using global parameters. For the emission of IMF's ( $Z$  greater or equal to 5) were calculated with the parabolic model approximation of barrier penetration, using the nuclear potential of Christensen and Winther [11].

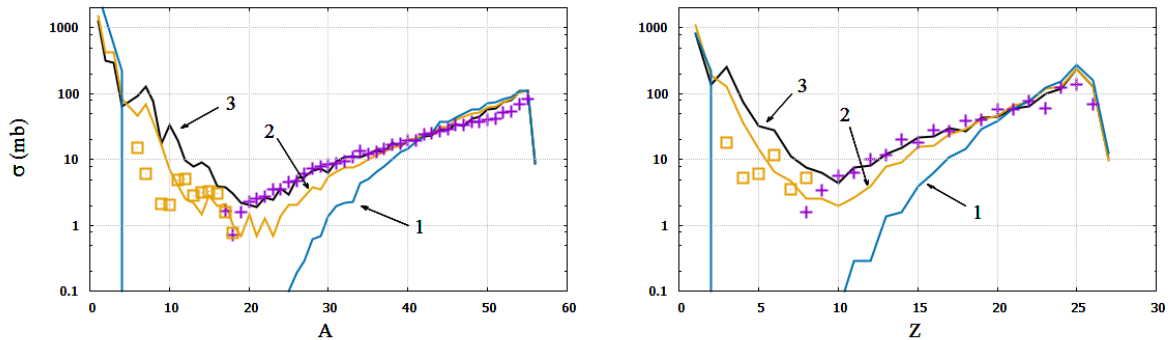


**Fig. 1** Mass and charge distributions of evaporation residues and intermediate mass fragments in spallation reactions of 1.0 GeV p +  $^{56}\text{Fe}$ . Experimental data (symbols) are compared with calculations performed with the code ISABEL followed by MECO (solid lines), as discussed in the text.

Figure 1 shows the mass and charge distributions of evaporation residues and intermediate mass fragments in 1.0 GeV p +  $^{56}\text{Fe}$  spallation reactions. Experimental data (symbols) [12,13] are compared with calculations performed with the code ISABEL followed by MECO (solid lines). Lines marked with number 1 refer to a calculation with MECO involving emission of gamma-rays, neutrons, protons and alpha-particles. This calculation agrees with the experimental data for  $A > 40$  and  $Z > 20$ , but fails to describe the data at lower  $A$  and  $Z$  values. A better overall agreement with the data is obtained if we include in the calculation the emission of IMF's with  $A$  up to 20 and  $Z$  up to 9. This amounts to a total of 42 decay channels. In this case, we obtain the curves marked with number 2, shown in Figure 1. We realize a significant improvement in the description of the data, in the whole range of  $A$  and  $Z$ . Finally, we examine the role of emitted fragments in excited-bound and excited-unbound states in the discrete and the continuum part of their energy spectrum. This amounts to a total number of 181 decay channels in our calculations with MECO. We obtain the curves marked with number 3 in Figure 1. We note that above  $A=20$  and  $Z=10$ , the  $A$ - and  $Z$ -distributions are well reproduced. At lower values of  $A$  and  $Z$ , the calculation overestimates the data. However, these distributions contain fragments emitted in particle-unbound states.

If we allow for the deexcitation of particle-unbound fragments, we end up with the final distributions shown in Figure 2. We realize a good overall agreement with the data for all values of  $A$  and  $Z$ . On the same Figure, the dashed curves show the results of a preliminary calculation with ISABEL-SMM. This calculation describes well the low and high regions in

$A$  and  $Z$  of both distributions. However, it severely underestimates the central regions. A tuning of the model parameters is in progress.

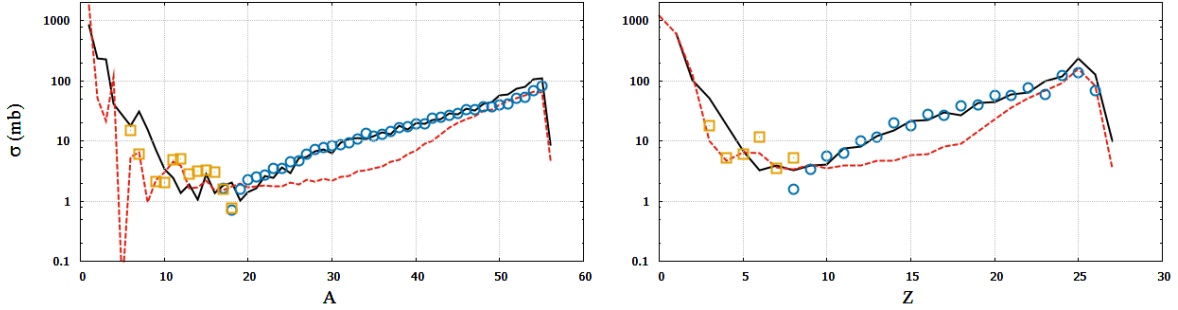


**Fig. 2** Mass and charge distributions of evaporation residues and intermediate mass fragments in spallation reactions of 1.0 GeV p +  $^{56}\text{Fe}$ . Experimental data (symbols) are compared with calculations performed with ISABEL-MECO (solid curve) and ISABEL-SMM (dashed curve).

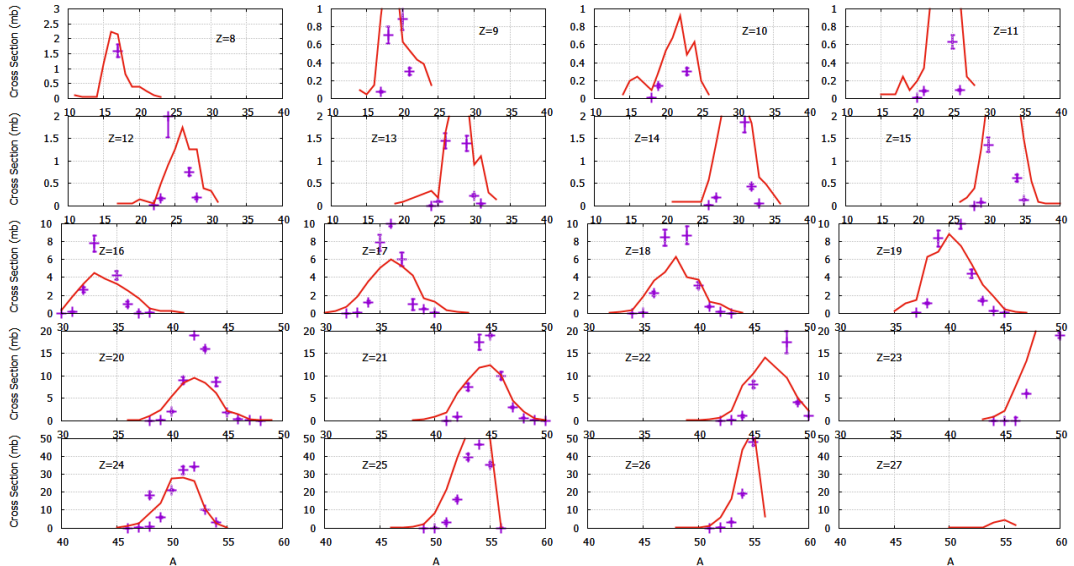


**Fig. 3** Isotopic distributions in spallation reactions of 1.0 GeV p +  $^{56}\text{Fe}$ , for the indicated values of  $Z$ . Experimental data (symbols) are compared with calculations performed with the code ISABEL followed by MECO (solid line).

In Fig. 3, we show the isotopic yields of spallation residues produced by p +  $^{54}\text{Fe}$  at 1.0 GeV. The experimental data [12] are shown with symbols and compared with calculations performed with ISABEL-MECO (solid curves). Note that the scales are linear. The calculations describe well the peak positions. However, the widths of the experimental distributions are slightly overestimated. Furthermore, the low- $A$  tails of the isotopic distributions of the heaviest residues with  $Z=25$  and  $26$  are slightly overestimated.

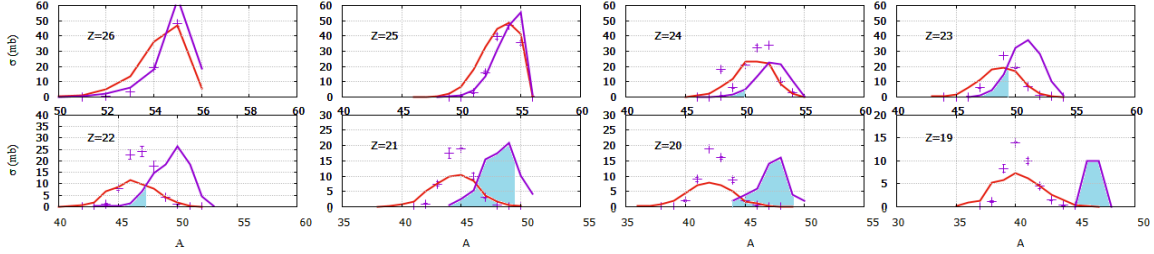


**Fig. 4** Isotopic distributions in spallation reactions of 1.0 GeV p +  $^{56}\text{Fe}$ , for the indicated values of Z.

Experimental data (symbols) are compared with calculations performed with the code ISABEL followed by MECO (thin solid lines). Thick solid lines show the primary distributions obtained with the code ISABEL. The shaded regions indicate portions of the distributions which would better deexcite with SMM.

In order to assess the importance of multifragmentation events in the mass, charge and isotopic distributions, we have examined the excitation energy distributions of the primary fragments from the calculation with ISABEL. The symbols in Figure 4 show the experimental isotopic distributions of spallation residues with Z=19-26. The thin curves are the calculated distributions with ISABEL-MECO. The thick curves show the corresponding primary distributions from ISABEL. The shaded regions of these distributions involve fragments with an excitation energy greater than 3 MeV/A. In other words, events in the shaded regions would better deexcite with SMM rather than with MECO. In such a case, they would feed the peak regions of distributions with Z=19-21, thus improving the agreement with the data. We are in the process of performing calculations involving events from both MECO and SMM, in order to study the influence of multifragmentation events on the experimental observables.

## SUMMARY AND CONCLUSIONS

In the present work, we combined the intranuclear cascade code ISABEL with the sequential binary decay code MECO as well as the code SMM in a study of spallation reactions induced by high-energy protons on  $^{56}\text{Fe}$ . Preliminary calculations 1.0 GeV were compared with experimental mass, charge and isotopic distributions. The calculations with ISABEL-MECO were based on a global level density parameter  $a=A/8$  and evaporation barriers for IMF emission calculated with the Christensen and Winther nuclear potential. They provide a good description of the mass and charge distributions. The centroids of the isotopic distributions were also well described by our calculations. However, the widths of the isotopic distributions were overestimated. It is very interesting that the majority of the data is described well with calculations based on a few simple assumptions. Refinements in the model parameters, such as the level density, are in progress. From the point of view of the ISABEL-SMM calculations, a tuning of the model parameters is needed, in order to estimate, if possible, the presence and contribution of multifragmentation events in the experimental observables.

## References

- [1] A. Krasa, *Spallation reaction physics, Neutron Sources for ADS, Prague, Rez. May 2010.*
- [2] R. Silberberg and C.H. Tsao, Phys. Rep. 191, 351 (1990)
- [3] J.C. David, Eur. Phys. J. A 51, 68 (2015)
- [4] Y. Yariv and Z. Fraenkel, Phys. Rev. C 20, 2227 (1979)
- [5] Y. Yariv and Z. Fraenkel, Phys. Rev. C 24, 488 (1981)
- [6] J.P. Bondorf, A.S. Botvina, A.S. Iljinov, I.N. Mishustin and K. Sneppepen, Phys. Rep. 257, 133 (1995)
- [7] A.S. Botvina, (INR, Moscow, Russia) *Role of multifragmentation in spallation reactions*, Proceedings of Joint ICTP-IAEA Advanced Workshop on Model Codes for spallation reactions, Trieste, Italy, 4-8th February 2008, arXiv:0806.3455 [nucl-th]
- [8] N. Eren, N. Buyukcizmeci, R. Ogul and A.S. Botvina, Eur. Phys. J. A 49, 48 (2013)
- [9] G. S. Soulis, A.S. Botvina et al., Phys. Rev. C 75, 044603 (2007)
- [10] N.G. Nicolis, Int. J. Mod. Phys. E 17, 1541 (2008)
- [11] P.R. Christensen and A. Winther, Phys. Lett. B 65, 19 (1976)
- [12] C. Villagrana-Canton et al., Phys. Rev. C 75, 044603 (2007)
- [13] P. Napolitani et al., Phys. Rev. C 70, 054607 (2004)